International Journal of Nanomedicine

Dovepress
open access to scientific and medical research

Open Access Full Text Article

ORIGINAL RESEARCH

Long-term biocompatibility of fluorescent diamonds-(NV)-Z~800 nm in rats: survival, morbidity, histopathology, particle distribution and excretion studies (part IV)

This article was published in the following Dove Medical Press journal:
International Journal of Nanomedicine

Frank C Barone[1]
Cezary Marcinkiewicz[2,3]
Jie Li[1]
Yi Feng[4]
Mark Sternberg[2]
Peter I Lelkes[3]
David Rosenbaum-Halevi[5]
Jonathan A Gerstenhaber[3]
Giora Z Feuerstein[2]

[1]SUNY Downstate Medical Center, Department of Neurology, Brooklyn, NY, USA; [2]Debina Diagnostic Inc., Newtown Square, PA, USA; [3]Department of Bioengineering, Temple University, College of Engineering, Philadelphia, PA, USA; [4]WuXi AppTec (Suzhou) Co., Ltd., China; [5]Texas University Health Center, TMC, Houston, TX, USA

Background: Thromboembolic events are a major cause of heart attacks and strokes. However, diagnosis of the location of high risk vascular clots is hampered by lack of proper technologies for their detection .We recently reported on bio-engineered fluorescent diamond-(NV)-Z~800nm (FNDP-(NV)) conjugated with bitistatin (Bit) and proven its ability to identify iatrogenic blood clots in the rat carotid artery in vivo by Near Infra-Red (NIR) monitored by In Vivo Imaging System (IVIS).
Purpose: The objective of the present research was to assess the in vivo biocompatibility of FNDP-(NV)-Z~800nm infused intravenously to rats. Multiple biological variables were assessed along this 12 week study commissioned in anticipation of regulatory requirements for a long-term safety assessment.
Methods: Rats were infused under anesthesia with aforementioned dose of the FNDP-(NV), while equal number of animals served as control (vehicle treated). Over the 12 week observation period rats were tested for thriving, motor, sensory and cognitive functions. At the termination of study, blood samples were obtained under anesthesia for comprehensive hematology and biochemical assays. Furthermore, 6 whole organs (liver, spleen, brain, heart, lung and kidney) were collected and examined ex vivo for FNDP-NV) via NIR monitored by IVIS and histochemical inspection.
Results: All animals survived, thrived (no change in body and organ growth). Neuro-behavioral functions remain intact. Hematology and biochemistry (including liver and kidney functions) were normal. Preferential FNDP-(NV) distribution identified the liver as the main long- term repository. Certified pathology reports indicated no outstanding of finding in all organs.
Conclusion: The present study suggests outstanding biocompatibility of FNDP-(NV)-Z~800nm after long-term exposure in the rat.

Keywords: nanocarbon particles, biocompatibility, liver toxicology, ex vivo IR organ imaging

Introduction

When combined, cardiovascular and cerebrovascular thromboembolic events (TEEs) account for the majority of deaths in the adult population in the developed world and contribute to >$400 billion in health care costs in the USA alone.[1–4] With this in mind, the ability to accurately and efficiently diagnose TEE would result in significant reduction in morbidity and mortality, as well as in the costs of managing devastating morbidities. To this end, diagnostic technologies that aid in risk assessment of predisposing conditions that underlie TEE are direly needed. Of particular importance in this regard are diagnostic methods that can be widely applied for preventive medicine surveys in ambulatory setting with high accuracy, safety, and

Correspondence: Cezary Marcinkiewicz
Department of Bioengineering, Temple University, College of Engineering, 1947 N. 12th St, Philadelphia, PA 19122, USA
Tel +1 267 215 204 3307
Email cmarcink@temple.edu

submit your manuscript | www.dovepress.com
Dovepress
http://dx.doi.org/10.2147/IJN.S189048

low costs. The current treatment guidelines for TEEs are guided by the interplay between our knowledge of disease pathophysiology[5] and the ability of our diagnostic tools to convey disease phenomena. As a result, clinical rationale is limited by the information our diagnostic tools can provide. While our mainstays of diagnostic imaging, such as computerized tomography, Magnetic Resonance Imaging (MRI), and contrast-based angiography, can provide invaluable information about TEE-associated disease process, they all share the shortcoming of lacking the resolution of directly portraying active clot particles. To directly label actual clot material would be invaluable in diagnosing thrombotic events in the acute phase, as well as screen for potential TEE waiting to occur. Moreover, the ability to recognize activated clot would allow physicians and medical scientists to bridge the gap between known mechanisms of disease pathophysiology and to recognize the disease process in real time, thus dramatically changing the diagnostic criteria and treatment protocols. From a purely diagnostic standpoint, a tool that could perform this task in a portable or ambulatory setting with little requirement for cumbersome hardware would allow for immediate diagnosis of TEE, or potential TEE, long before a patient could arrive at the hospital. An exhaustive review of the potential applications for technology that would allow for direct visualization of clot material is beyond the scope of this paper; however, we will mention a few for the sake of illustration.

The diagnostic criteria for intervention in carotid artery disease have not changed significantly since the publication of the NASCET and ESCET trials which rely primarily on defining percent of vessel stenosis and morphology revealed by carotid ultrasound (US) or angiography for patient stratification and, thus, treatment recommendations.[6–10] However, our knowledge of atherosclerotic disease mechanisms reveals a multifactorial process of clot formation and rupture, and still the phenomenon of TEE event is known to commonly occur in low-risk cases, even though in the absence of a clear etiology; these events are labeled "cryptogenic" as they do not conform to the diagnostic criteria established by trial guidelines.[11–13] The ability to directly visualize clot would thus allow for new disease stratification that will result in more accurate diagnosis and treatment algorithms, and a tool that could accomplish this task in an ambulatory setting would prove invaluable. Of course, a similar utility could be applied to risk stratification and management of coronary disease, and could even be employed by first responders in the field, in order to immediately diagnose acute coronary occlusion without the confounders associated with electrocardiogram and cardiac enzymes, facilitating appropriate treatment and triage to vessel catheterization.

It is not uncommon for a patient to be admitted for diagnostic work-up for acute cerebral TEE, without successful identification of clot etiology. These events are referred to as "cryptogenic"[14–17] stroke; appropriate medical management of these cases presents a great clinical challenge and, as such, is the subject of multiple clinical trials. Most recently, the ARCADIA trial attempts to define the ideal empiric management in stroke under the presumption of atrial fibrillation as the stroke etiology without diagnostic evidence of cardiogenic source.[18] Being able to directly visualize thrombotic material in the heart and large cervical vessels would enable accurate diagnosis of stroke etiology, and thus result in safe and effective treatments, and such a tool would have significantly higher resolution of detecting a clot than the current diagnostic modalities of US and MRI applied in these cases. Currently, patients in this clinical setting are treated presumptively based on indirect diagnostic findings such as patent foramen ovale and can be subject to potentially hazardous anticoagulation, or even surgical procedures, that could be avoided.[19,20]

Finally, diagnostic tools that would allow direct clot visualization could be integrated into current imaging modalities, providing a significantly more accurate picture of TEEs and an aide to the operator performing interventional techniques.

We have recently reported on bioengineering of fluorescent nanodiamond particles with NV active centers (FNDP-[NV]) linked covalently to the disintegrin protein bitistatin.[21] This bioengineered construct was designed to selectively co-junction with the human integrin platelet fibrinogen receptor (PFR, αIIbβ3 receptor). Since αIIbβ3 is the most abundant platelet adhesion molecule, which in its activated state promotes binding to fibrinogen, we postulated that bitistatin attached to FNDP-(NV) could be positioned via its ligand in blood clots, and hence help in their identification via the presence of the FNDP-(NV) particles upon the latter's propensity to emit near-infrared (NIR) upon excitation. We have demonstrated that FNDP-(NV)-Z~800/Bitistatin binds with high avidity to activated PFR in vitro and further by its association with platelets within a platelet-rich plasma clot ex vivo.[21] The key data serve as proof of concept (POC) of the core hypothesis. We then proceeded to test our hypothesis further in in vivo conditions such as blood clot formation induced by lesions at the luminal surface of the carotid artery bifurcation zone of anesthetized rats[22] and demonstrated the ability to record NIR extra-corporeally via the in vivo imaging system (IVIS), further confirming the association

of particles with blood clots localized on vascular lesion via fluorescent microscopy of the vessels. In addition, we quantitated particles extracted from the isolated blood clots.[22]

Equipped with POC that FNDP-(NV)-Z~800/Bitistatin complies with its intended design, we conducted a pilot safety, tolerability, and organ distribution study in conscious rats.[23] In this acute/subacute study, particles were administered by brief intravenous infusion (single dose of 60 mg/kg) and followed for 5 or 14 days for a variety of safety and biocompatibility variables. These pilot studies revealed no mortality or morbidity as well as essential organ distribution (liver, spleen lung, heart, and kidney). Since these pilot studies[23] might not comply with the likely regulatory requirements for prolonged safety and Absorption, Distribution, Metabolism, and Excretion and toxicology evaluations, we now report on a follow-up study conducted over 12 weeks following the same study design, yet with expanded monitoring of particle distribution, safety biomarkers, histopathology, particle excretion, hematological evaluation, and blood biochemistry. The information generated in this 12-week study is presented in this manuscript.

Materials and methods

Preparation of nanoparticles for in vivo studies

FNDP-(NV) functionalized with carboxyl moieties were purchased from ADAMAS Nanotechnologies (Raleigh, NC, USA). FNDP-(NV) were then sterilized by immersion in 70% ethanol (Decon Labs Inc., King of Prussia, PA, USA) for 30 minutes. Particles were isolated by centrifugation, supernatant was removed, and the particles were washed once with sterile PBS. The sterile particles were further blocked by sterile PBS containing 3% of BSA.[23] The properties of FNDP-(NV), such as dynamic light scattering and zeta potential, were stable and were controlled as described previously.[23]

In vivo studies: animal husbandry and surgery

All animal procedures were performed according to the guidelines of the US Animal Welfare Act and approved by the Institutional Animal Care and Use Committee at SUNY Downstate Medical Center, NYC (Association for Assessment and Accreditation of Laboratory Animal Care International accredited). Adult male Sprague Dawley rats weighing 350 g±10% of the body weight (Charles River Laboratories, Wilmington, MA, USA) were maintained on a 12-hour light–dark cycle and were given ad libitum access to standard lab chow and tap water.

Surgery was conducted under anesthesia using 4%–5% isoflurane (IF) for induction followed by 1%–2% IF (maintenance) adjusted throughout the procedure. Rats were held in the supine position and subjected to surgery aided by binoculars under aseptic conditions. A PE-10 cannula was inserted into the left femoral vein for infusion of FNDP-(NV) particles or vehicle PBS (vehicle control). Particles were suspended in 2 mL PBS and vortexed immediately before loading into 5 mL syringe. FNDP-(NV) or PBS (control) infusion was completed over 2–3 minutes (Figure 1A).

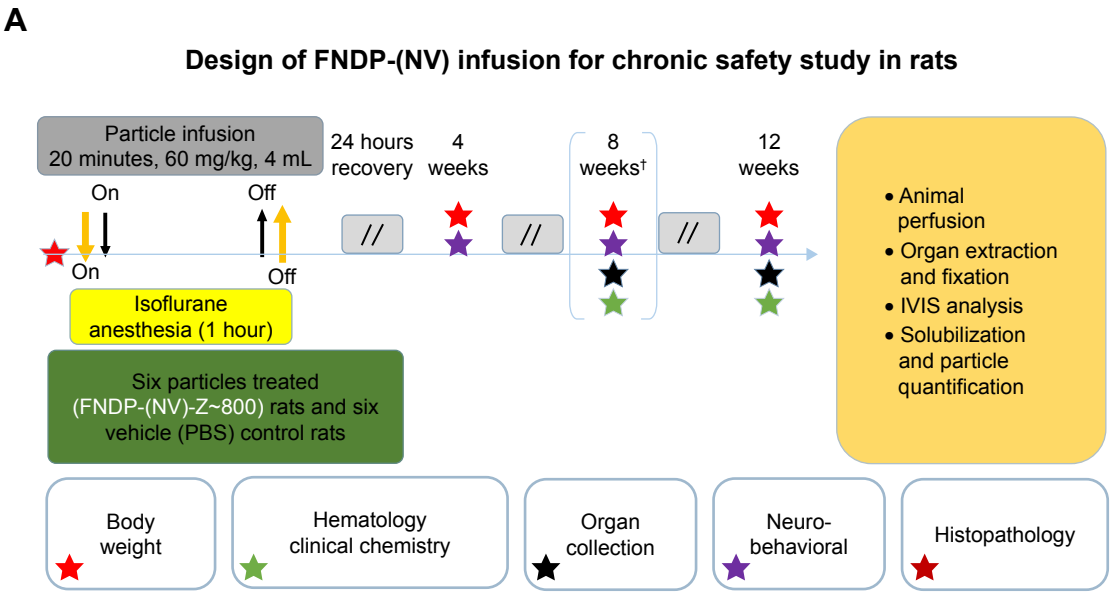

Figure 1 (*Continued*)

B

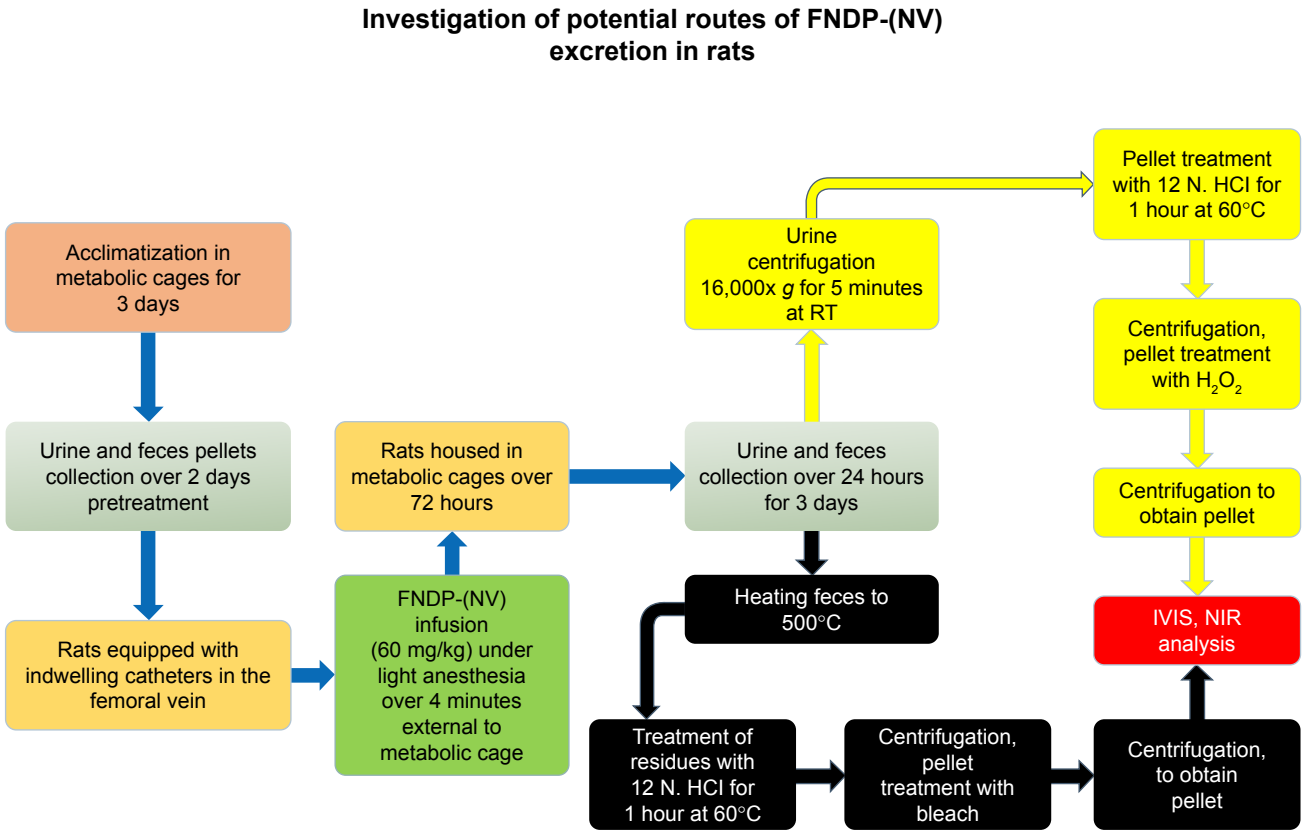

Figure 1 The schematic design of studies performed in reported investigations.
Notes: (**A**) The scheme describes the design of the 12-week study performed in vehicle controls and FNDP-(NV)-treated rats. Boxes denoted with colored stars report on the assays performed along the 12-week study at various time points as illustrated by the color of the stars. Day 1 denotes the onset of study commencing with gas anesthesia and treatments as written in the box above. Bracketed star cluster on day 60 marked by an asterisk denotes the terminal activities performed on the vehicle control group, while the particle-treated group proceeded to 90 days when same studies were done. Double-forward slashes denote non-continuous time intervals between tests. (**B**) The scheme describes the protocol for treatment of rats with F-NDP-(NV) to investigate the excretion of particles by urine and feces. FNDP-(NV) denotes the FNDP-(NV)-Z~800 used in all studies.
Abbreviations: FDNP-(NV), fluorescent nanodiamond particles with NV active centers; IVIS, in vivo imaging system; NIR, near infrared; RT, room temperature.

Organ collection and preservation for histopathology inspection

At the end of the protocol (8 weeks for control and 12 weeks for FNDP-[NV]-treated), rats were anesthetized with 5% IF for deep hypnosis and the abdominal aorta was quickly isolated and cut to allow blood drainage by free flow. Thereafter, the exsanguinated animals were perfused (10 mL) with sterile saline to minimize residual blood in organs, followed by infusion of preservation solution of 4% paraformaldehyde in saline. Organs were carefully dissected, suspended in excess of 10% neutral buffered formaldehyde, and preserved for histopathology processing and ex vivo NIR fluorescence evaluation (n=6).

Tissue processing for histopathology analysis

All organs collected for tissue histopathology analysis (six sets each containing liver, spleen, heart, kidney, and lung) were processed by certified pathologists at WuXi AppTec (Suzhou, China) a contract research organization (CRO). The facility is fully compliant with the USA Food and Drug Agency (FDA), Organization for Economic Co-operation and Development, and China Food and Drug Administration. The pathology evaluation was conducted in accordance with the certified Standard Operating Procedures (SOPs) in China. All organs were received in acceptable condition in vials with excess 10% NBF. Each tissue was trimmed as per WuXi AppTec SOP into appropriately labeled embedding cassettes (sectioning and embedding formats as presented in Figure S1). Tissues were processed with a Leica ASP300 processor and embedded in paraffin with a Leica Histocore Arcadia H/C. Each tissue was then sectioned at 5 µm with a Leica RM2235 microtome and stained with H&E with a Leica Autostainer XL (Leica Microsystems, Wetzlar, Germany).

Ex vivo analysis of NIR emission by whole organ using IVIS and quantification of extracted FNDP-(NV) by spectrofluorometry

NIR fluorescence imaging of whole organs was carried out by an IVIS (IVIS 50 Imaging System; PerkinElmer Inc., Akron, OH, USA) using the same parameters as described previously.[23] Briefly, the instrument was set up at 580–610 nm for excitation and 695–770 nm for emission bandpass filters, with 5-second exposure, "binning" set at 4, and a 10 cm field view, as reported previously.[23] Autofluorescence was subtracted based on excitation at 445–490 nm under otherwise identical imaging conditions. For each organ, the mean fluorescence intensity of the image, adjusted for autofluorescence, was evaluated using proprietary IVIS software. Extraction of FNDP-(NV) from different organ tissues was performed as described previously.[22] Briefly, organs were cut into 0.2–0.3 cm pieces and immersed in 12 N HCl and incubated overnight at 60°C. Particles were separated from the soluble residues by series of centrifugations, decantation, and resuspension in deionized (DI) water. Samples containing particles from solubilized organs and normalized standards were applied on the same 96-well plate and read in the Tecan plate reader (Tecan AG, Männedorf, Switzerland) using NIR fluorescence filters (excitation 570 nm, emission 670 nm).

The schematic protocol for rat treatment, collection of feces and urine, and sample preparation for IVIS analysis is presented in Figure 1B. The in vitro part of the study was done at WuXi AppTec NJ, a USA subsidiary of WuXi AppTec China. Each rat was housed in a metabolic cage (Hoeltge Inc., Cincinnati, OH, USA) where separation of urine from feces excrements allows collection of each medium into separate collection bins. Collection commenced 2 days prior to test FNDP-(NV) or control (PBS) infusion and designated pre-collection period, followed by 3 days of 24-hour cycle of urine and fecal pellet collection. Rats (320 g) were injected with FNDP-(NV) (60 mg/kg) in 4 mL PBS over 4 minutes through an indwelling catheter in the femoral vein. Each collected sample was stored separately at 4°C until further processing and analysis by IVIS.

Fecal analysis

Fecal pellets (2.4 g) taken from each time point of the collection period of 24 hours were exposed to 500°C for 30 minutes in a Barnstead Thermodyne type 1400 furnace oven (Barnstead Thermolyne Corp., Ramsey, MN, USA) in order to eliminate the organic materials. This step aimed to reduce background NIR interference with the FNDP-(NV) signal and the mass of organic materials by 90%. Residual ashes (10% of the original sample) were suspended in 6 mL of 12 N HCl and incubated at 60°C for 1 hour. Samples were centrifuged using 16,000× *g* force for 5 minutes at room temperature. Supernatant was discarded, and the pellets were washed with 6 mL of DI water and centrifuged as above. Pellets were treated with 6 mL of commercial bleach (Clorox®) containing 6% of sodium hypochlorite (active ingredient) and incubated overnight at 60°C. Samples were centrifuged as above, and the pellets were washed with DI water and analyzed by IVIS with filter setting of 580–610 nm for excitation and 695–770 nm for emission, with 20-second exposure, "binning" set to 2, and a 12×12 cm field of view.

Urine analysis

Urine samples were centrifuged at 16,000× *g* for 5 minutes at room temperature. Pellets were treated with 1 mL of 12 N HCl and incubated for 1 hour at 60°C. Samples were centrifuged as above, and the pellets were washed with 1 mL of DI water and centrifuged again. Pellets were treated with 1 mL of 30% H_2O_2 by overnight incubation at 60°C. Tubes were recentrifuged and washed as above, and analyzed using IVIS setting, as described above for feces, using 10-second exposure time.

Neurobehavioral tests

The set of motor and sensory functions deployed in this study have been described and referenced in great detail.[23–25] In the 12-week study, an additional test for cognitive function was added.

Active place avoidance (APA) learning test

APA was measured at 4 and 8 weeks post-PBS injection (control) and 4, 8, and 12 weeks after FNDP-(NV) administration. The tests were conducted as previously described.[24,25] Each rat experienced an even number of 10-minute trials on a slowly rotating circular behavioral arena that monitored entry into an invisible (computer-controlled) 60° stationary quadrant on the floor of the arena where electrical shock was applied (the "shock avoidance zone"). Rats were tracked by a programmed video "spot-tracker" computer (wireless camera) mounted above the arena (BioSignal Group, Brooklyn, NY, USA). Upon entry into the shock avoidance zone, a mild foot shock was delivered to the rat by a pulse of constant current (0.3 mA, 60 Hz, 500 ms). The number of shocks (Negative Reinforcements), the number of entrances into the shock zone (Entrances), and the time

in seconds to enter the shock zone (Time to First Entry) in each 10-minute trial were measured. The total path distance in meters traveled by the rat over the test period was also recorded (serves to calculate an index of motor activity per 10-minute trial).

Hematology and biochemistry tests

Under deep anesthesia, blood was collected via cardiac puncture into citrated vials (at 9:1 ratio) at the designated end points of the experiment and analyzed on the same day for blood hematology and biochemistry analysis. The assays were done by standard methods at the State University Downstate Hospital, Clinical Laboratory Service, Brooklyn, NYC, NY. Due to shortage of blood acquisition, some assays were conducted only in one or two animals.

Statistical analyses

Data are presented as mean ± SD. Statistical analyses were done by ANOVA (where appropriate) and Student's *t*-test (one or two tailed as noted) using SigmaPlot software (SigmaPlot® 12 SPSS; Systat Software Inc., San Jose CA, USA). Statistical significance was established at $P<0.05$ for the number of independent studies performed.

Results

Due to logistics limitation in laboratory capacity, the control (PBS) group was terminated on the eighth week while the test article group was allowed to proceed to the prespecified termination time of 12 weeks. None of the animals in the study had succumbed during the study duration, and no changes in appearance or gross aberrant manifestations were identified by visual inspection.

Evaluation of body and organ weights

Body weights of FNDP-(NV) – and PBS (control)-treated rats are presented in Figure 2. All animals gained weight and no differences were noted between the control and FNDP-(NV)-treated rats ($P=0.282$, two-tailed Student's *t*-test; Figure 2A). Comparison of the weights of five organs (liver, spleen, heart, kidney, and lung) was performed as per 100 g of total body weight at the time point of organ collection. No statistical difference was noted across the control- and FNDP-(NV)-treated animals (Figure 2B). Visual inspection of organ surface failed to identify necrosis, hemorrhages, or gross contour changes (photos available upon request).

Effects of FNDP-(NV) on blood cell count and biochemistry

Blood analyses are depicted in Figure 3 (Table S1). No difference in any assay was noted between the control and particle-treated animals. Of special importance are normal liver (ALP, AST, ALT) functions and normal kidney (creatinine and blood urea nitrogen) functions, indicating sufficient organ integrity at the end of the experimental period. Moreover, coagulation biomarkers (International Normalized Ratio, prothrombin time, activated partial thromboplastin time, fibrinogen) were not affected by the exposure to FNDP-(NV).

IVIS imaging of whole organs

IVIS images of whole organs conducted at the end of the experiment are presented in Figure 4. Only the liver and spleen of the FNDP-(NV)-treated rats had increased signal over background that showed a significance at $P<0.001$ for liver and $P<0.01$ for spleen (n=6) in statistical analysis. Representative images

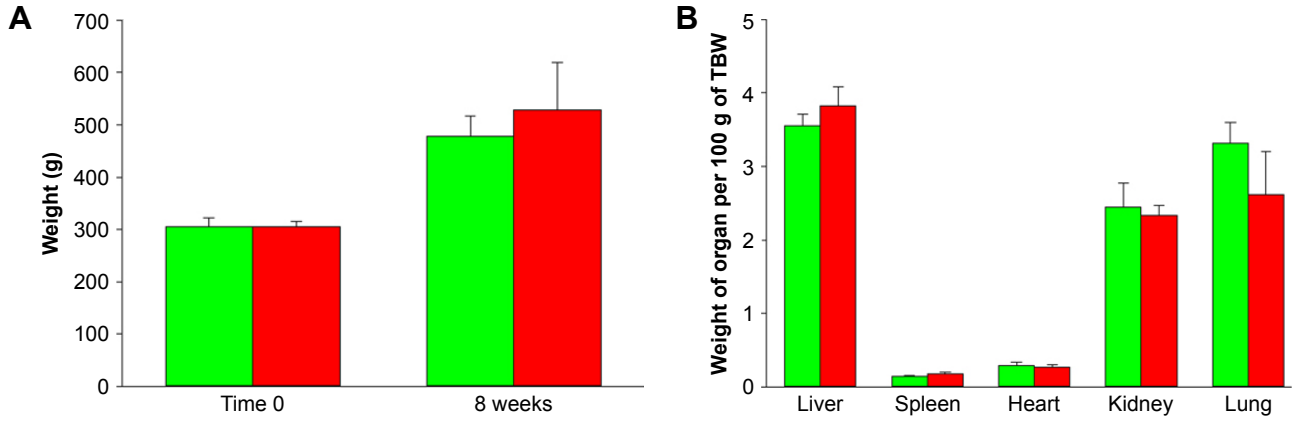

Figure 2 Body and organ weights of the vehicle control (green)- and FNDP-(NV)-treated (red) rats prior to the onset of the study and at its termination.
Notes: (**A**) Comparison of rats' body weights at baseline and after 8 weeks of progression of experiment. (**B**) Comparison of organ weights after 8 weeks (control) and 12 weeks (FNDP-(NV) treated) of treatment, expressed as per 100 g of the total body weight. Error bars represent SD for the control group (n=5) and the FNDP-(NV) group (n=6). There was no significance difference between the control and FNDP-(NV) groups ($P>0.05$, two-tailed Student's *t*-test).
Abbreviations: FNDP-(NV), fluorescence nanodiamonds particles with NV active centers; TBW, total body weight.

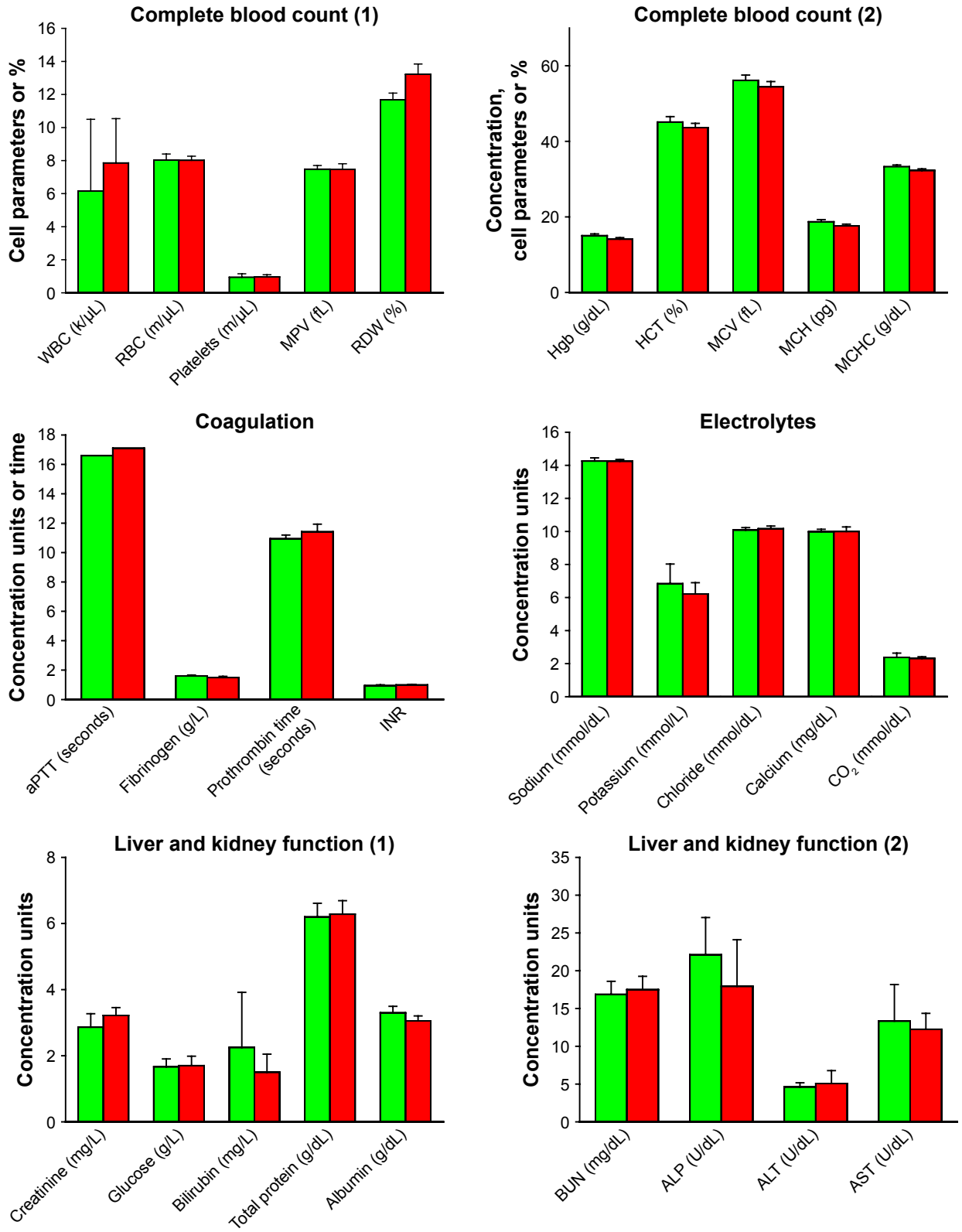

Figure 3 Analysis of different blood parameters of investigated rats.

Notes: The green bars represent controls (PBS treated) and the red bars represent FNDP-(NV)-treated animals. n=8 for the control group and n=6 for the particle-treated group in "electrolytes" and "liver and kidney function" analysis; n=7 for the control group and n=6 for the FNDP-(NV) group in "complete blood count" analysis; n=5 for the control group and n=6 for the FNDP-(NV) group for fibrinogen, prothrombin time, and INR analysis; n=1 for the control group and n=2 for the FNDP-(NV) group for aPTT analysis. No statistical significance was observed between the control (PBS) and FNDP-(NV)-treated groups (two-tailed Student's *t*-test, $P>0.05$).

Abbreviations: aPTT, activated partial thromboplastin time; BUN, blood urea nitrogen; FNDP-(NV), fluorescence nanodiamond particles with NV active centers; Hgb, hemoglobin; HCT, hematocrit; INR, International Normalized Ratio; MCH, mean corpuscular hemoglobin; MCHC, mean corpuscular hemoglobin concentration; MCV, mean corpuscular volume; MPV, mean platelet volume; RBC, red blood cells; RDW, red cell distribution width; WBC, white blood cells.

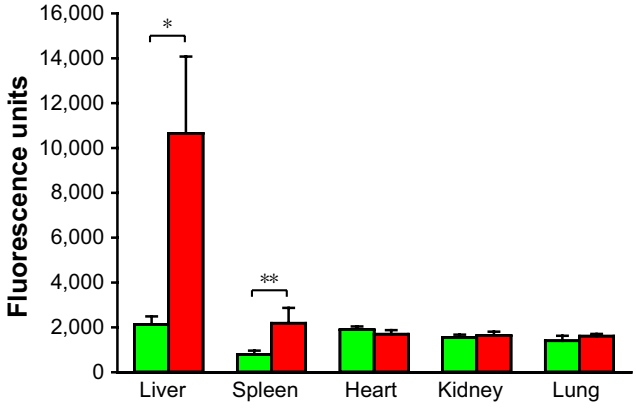

Figure 4 Fluorescence intensity of whole organs isolated following study termination.

Notes: Green bars represent animals treated with vehicle (PBS) that served as controls, and red bars represent FNDP-(NV)-treated rats. Error bars represent SD for n=6. *$P<0.001$, **$P<0.01$ compared to the control group by two-tailed Student's *t*-test.

Abbreviations: FNDP-(NV), fluorescence nanodiamond particles with NV active centers; IVIS, in vivo imaging system.

of the organs analyzed by IVIS are presented in Figure S2. Kidneys, lungs, and hearts obtained from treated animals had no increase in NIR signal over that in the controls where no particles were infused. In addition, we inspected by IVIS four whole brains obtained from acute FNDP-(NV)-exposed rats kept for 5 or 14 days. As shown in Figure S3A, no specific NIR signals (over background) could be identified. Moreover, histochemical analysis of brain sections failed to reveal particles throughout the section (Figure S3B).

Quantification of extracted particles from solubilized organs

Direct analysis of FNDP-(NV) in rats' organs performed by measurements of NIR fluorescence of particles extracted from solubilized tissues and evaluated by using a Tecan spectrofluorometer instrument is presented in Figure 5A and B.

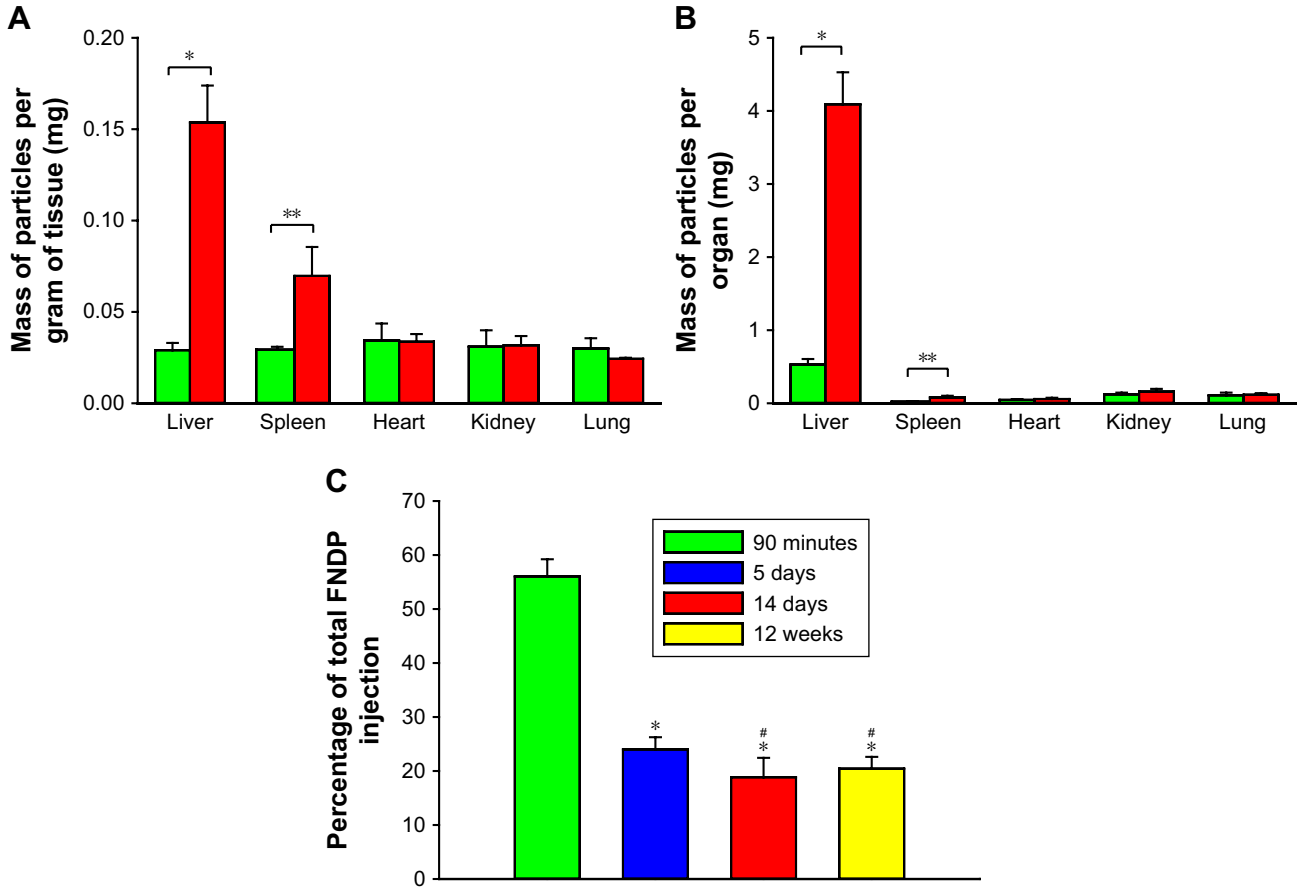

Figure 5 Comparison of quantities of FNDP-(NV) in solubilized organs collected in different time points of studies.

Notes: (**A**) Comparison of masses of FNDP-(NV) stratified per gram of organ weight for 12-week study. (**B**) Comparison of total masses of FNDP-(NV) in the whole organ for 12-week study. Green and red bars represent vehicle (PBS)- or FNDP-(NV)-exposed rats, respectively. Error bars represent the SD for n=3 per investigated group. *$P<0.001$, **$P<0.05$ for two-tailed Student's *t*-test. (**C**) Comparison of accumulation of FNDP-(NV) in the liver for different time points of studies. Percentage of accumulation was calculated based on the initial, total injection of particles (20 mg per rat). Data for 90 minutes, 5 and 14 days were adopted from a previous publication.[23] *$P<0.001$ vs 90 minutes for two-tailed Student's *t*-test. #$P<0.05$ vs 5 days, $P=0.81$ for day 14 vs 12 weeks for one-way ANOVA (Holm–Sidak method).

Abbreviation: FNDP-(NV), fluorescence nanodiamond particles with NV active centers.

The data clearly indicate that the liver was the prime organ of particle deposition. Significant particle load was also detectable in the spleen of FNDP-(NV)-treated animals. No differential signals were noted in the hearts, kidneys, and lungs as compared to their PBS controls. Noteworthy is the burden of particles in the liver (Figure 5C, yellow bar) that seems to be in par with the levels found at the end of the 5- and 14-day studies. The total amount of FNDP-(NV) found in the liver calculated as percent of the loading dose was 55.1%±3.1% following 90 minutes of FNDP-(NV) infusion, 24.0%±2.2% after 5 days, 18.8%±3.6% after 14 days, and 20.0%±2.2% after 12 weeks. Particles found at the end of the experiments done over 5 days, 14 days, and 12 weeks were statistically significantly different from the ones at 90 minutes ($P<0.001$). The percent of particles accumulated in the liver 12 weeks after exposure was not statistically different than that of particles in 14-day study ($P=0.809$). Furthermore, the percent of particles still residing after 14 days or 12 weeks was statistically significant from the 5-day residual depot (data for 90 minutes, 5 and 14 days were taken from Barone et al[23] for the sake of comparison).

Quantitation of particles in urine and feces

The assays deployed for monitoring FNDP-(NV) in the urine and feces did not yield consistent data to support the presence of particles in these biological specimens. As shown in Figure 6A (feces) and 6B (urine), the emission of NIR from urine or feces specimen generated equaled NIR intensities in the pre-exposure and post-exposure collection periods; in fact, if any, the average (pink columns) of the pre-exposure and post-exposure NIR emission obtained in the urine samples was slightly lower in the post-exposure days.

Neurobehavioral and cognitive studies

The APA learning paradigm displayed by number of times mice entered the "shock zone" and the number of shocks received is displayed in Figure 7. Analysis by four-way (treatment, time [week], trial, animal) mixed-model ANOVA demonstrated learning as evaluated by a reduction in significance ($P<0.001$) in the trial and week/time interaction. The asterisk in the graph indicates significant reduction (by *t*-test) of the seventh trial vs the first trial, denoting learning experience in both groups across the experimental period. Interactions of the week/time and treatment were not significant, indicating that treatment with FNDP-(NV) did not result in detectable alteration of learning capabilities. The entire expanded APA data set including additional test variables is presented in Table S2.

Several sensory and motor tests (described in detail in our recent publication[23]) were also conducted in this long-term study, including modified Neurologic Severity Score; foot fault; hind-limbs, beam balance, self-suspension time, and angle of sustained balance, as described before.[23] No differences were observed between the groups, and no deviation

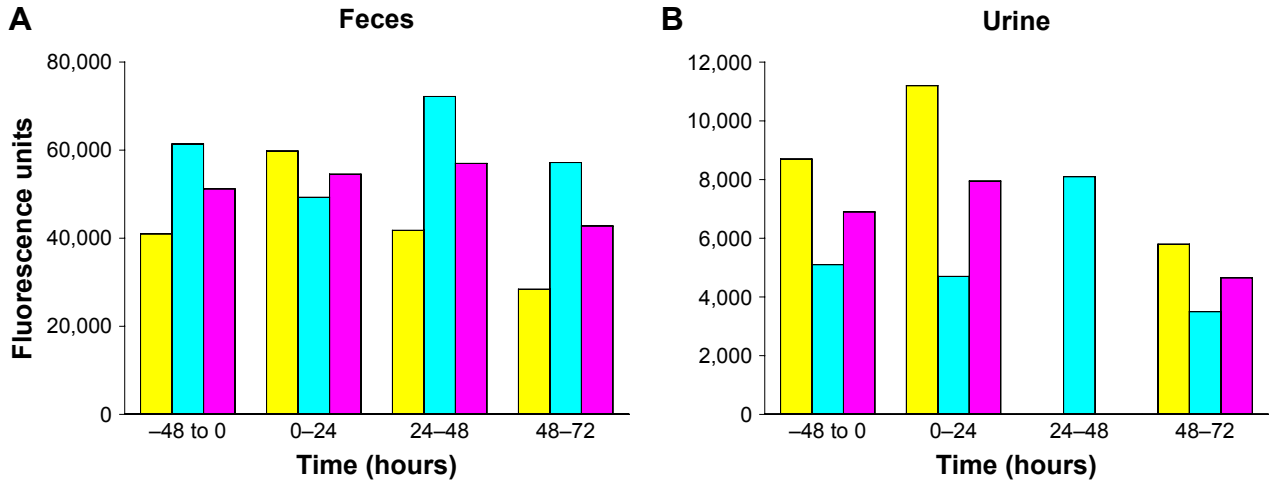

Figure 6 Detection of FNDP-(NV) in rat urine and fecal samples obtained before infusion (–48 to 0) and in different time points after infusion, using IVIS instrument.
Notes: (**A**) The graphic presentation of total intensity of fluorescence measured for indicated fecal samples collected in different time points. Yellow bars represent rat 1, cyan bars rat 2, and pink bars represent the mean from two rats. (**B**) The graphic presentation of total intensity of fluorescence measured for indicated urine samples collected in different time points. Yellow bars represent rat 1, cyan bars rat 2, and pink bars represent the mean from two rats. Background (vehicle) fluorescence was deducted from measured sample values. Value obtained for rat 1 urine sample in 24–48-hour time point was omitted due to technically faulty collection.
Abbreviations: FNDP-(NV), fluorescence nanodiamond particles with NV active centers; IVIS, in vivo imaging system.

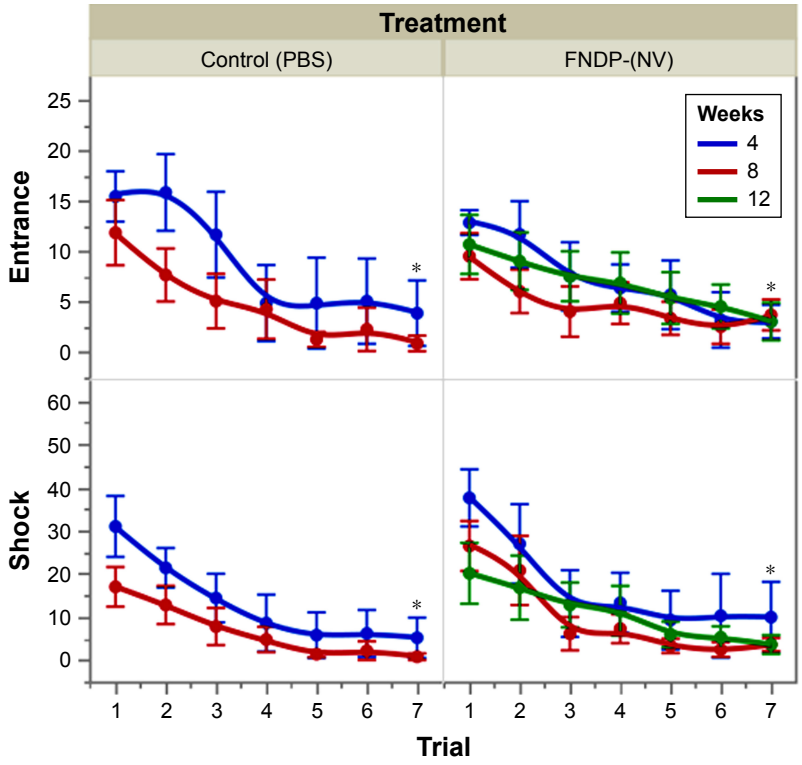

Figure 7 APA tests to compare the effect of FNDP-(NV) on the learning ability of rats.
Notes: Tests were performed after 4, 8, and 12 post-injection weeks. Control groups received sham (PBS) injection. Error bars represent SD for n=6. *$P<0.01$ compared to trial #1 (two-tailed Student's *t*-test).
Abbreviations: APA, active place avoidance; FNDP-(NV), fluorescence nanodiamond particles with NV active centers.

from normal performance was noted. These data are not included here, but are available upon request.

Histopathology results

The results of each of the analysis of the 30 organs of the six rats (three control and three FNDP-(NV)-treated) are presented individually to provide authentic view of the histopathology of each organ from each group. Furthermore, we have deposited the pathology report (received from the CRO, WuXi AppTec) in the Supplementary materials section III. Table 1 presents the incidental observation in a few rats by standard scoring method used by the pathologists. Overall, the two independent pathologists reading the slides indicated that there were no test article-related adverse findings in any of the organs. Reports on incidental histopathologic observation unrelated to specific drug treatment have been known in the species.[26,27] The incidental observation in the organ studies at WuXi AppTec includes a single mononuclear cell in the left ventricle, single hyaline deposition in one collecting duct in the kidney medulla, and mild pigmentation zone in the spleen (suspected as hemosiderin). Arrows pointing to these incidental findings are provided in the respective images of Figure S4.

Discussion

This investigation is a direct continuation of our recent pilot study exploring the acute biocompatibility of FNDP-(NV) in rodents.[23] The pilot studies suggested several important features that commanded extended and expanded investigations to cement the path for Good Laboratory Practices (GLP)

Table 1 Histopathology data of rats treated or not with FNDP-(NV)

Organ	Group of tested animals and animal number					
Type of pathology	Control (PBS)			FNDP-(NV) treated		
	1	2	3	1	2	3
Heart						
Mononuclear cell infiltration, focal	–	–	–	–	–	1+
Liver	–	–	–	–	–	–
Spleen						
Pigmentation (resembles hemosiderin)	–	–	–	–	1+	–
Lung	–	–	–	–	–	–
Kidney						
Cast, hyaline, focal	–	–	–	–	1+	–

Abbreviation: FNDP-(NV), fluorescence nanodiamond particles with NV active centers.

preclinical development of FNDP-(NV) toward Investigational New Drug (IND) submission as per FDA guidance. The primary requirement prior to commencing safety and biocompatibility studies in humans is animal safety and toxicology studies over extended periods over our past studies. The importance of the present manuscript resides in addressing potential impact of persistence of FNDP-(NV) particles in the major organs (liver and spleen) over prolonged post-exposure (12 weeks). Since the intended medical application of the technology (as detailed in the "Introduction" section) will require systemic exposure (intravenous infusion), we chose 12 weeks as a reasonable time frame to test the long-term consequences of particle deposition in key essential organs. As such, the present investigation is (to the best of our knowledge) the first of its kind where the strain of FNDP-(NV) particles and the size of particles (Z-average 700/800 nm) were tested.

The main conclusion of the 12-week safety study presented in this manuscript can be summarized as follows: 1) neither mortality nor morbidity (adverse effects) have been noted throughout the study; 2) FNDP-(NV) remain entrapped in vivo largely in the liver and to a lesser amount in the spleen; other organs of interest (heart, lung, kidney, and brain) had no identifiable particle deposits; 3) in spite of the prolonged entrapping of particles in the liver and spleen, no specific histopathologic observation was noted in these organs after 12 weeks; 4) no aberrant hematological cell count or biochemical biomarkers of liver and renal functions were detected; and 5) several tests of central and peripheral nervous systems were unaltered as evident by several sensory, motor, and cognitive tests.

It is, however, important to note that failure to observe particles in the kidney, lung, heart, and brain cannot absolutely exclude the possibility of minute presence of particles in these organs. The ability of the IVIS system to report on NIR emission is restricted by the critical mass of FNDP-(NV) in the organ and the ability of the NIR energy to transverse tissue absorption. These factors could lead to "false-negative" results, and therefore, we hold this technical issue as a main caveat in excluding the possibility that these organs do not retain particles. The IVIS-based data are further supported by spectrofluorescence studies (Tecan system) of the extracted particles from solubilized organs. Only liver and spleen extracts displayed evidence for the presence of particles. Since this latter technique virtually eliminates the organic material that might have interfered with NIR emission, we believe that the mass of particles in heart, lung, brain, and kidney might be below the capacity to emit NIR energy that can be detected by either method. In our recent study[23] (acute studies), we reported on fluorescent microscopy examination of 5 μm thick slices prepared from the heart, brain, lung, and kidney of FNDP-(NV)-treated rats, where only sporadic particles were observed. While we did not pursue this technology in the present study, we assume the same for the present one. It is noteworthy that at the end of the experimental period, about 80% of the injected dose could not be accounted for in the five organs monitored, suggesting that the bulk of the dose settled in the rest of the body, such as fat tissue, muscle, skin, and bone. Future studies are required using FNDP-(NV)-BSA-I[1,25] for more comprehensive, total body pharmacokinetics and distribution.[28] It is, however, noteworthy that our data are in line with the recent publications on distribution of nanodiamond particles infused into the systemic circulation of rodents (mice and rats), all reporting the liver and spleen as the main organs where nanodiamond particles are deposited.[28–30]

The literature concerning safety, toxicology, and distribution of nanocarbon particles has been extensively contested in recent reviews[31–33] and is beyond the scope of discussion regarding the particular nanodiamond particles studied by the authors. However, it suffices to point out that particle size[34] and surface additives (or "coronation") are expected to impact on biodistribution.[35–37] These variables are important factors in the literature's diversity on the subject of particles' biodistribution in vivo. In this regard, the FNDP-(NV) deployed in our study are BSA blocked in contrast to nanodiamonds reported elsewhere. Furthermore, although the FNDP-(NV) used in this study have no precedence in the published literature (to the best of our knowledge) and several attributes of the FNDP-(NV)-Z~800 nm are unique, the safety and distribution pattern presented in the present study closely follow a previously published report on long-term exposure.[29] In this latter reference, detonation nanodiamonds lacking "color centers" and of Z~100 nm were systemically infused to either rats or non-human primates. While the study in the former species (rat) was much shorter (2 weeks only), the non-human primate study extended repeated exposures over 6 months; yet, none reported adverse consequences to the particles exposed animals.

With this in mind, we recognize the need to ultimately explore much longer post-exposure periods likely at a scale of years. Also, reaching clear maximal tolerated dose will allow for rationalization of toxicology risks throughout long-term exposure against short-term benefits. Taken together, our 12-week study period strongly suggests that this strain of nanodiamonds might carry limited, if any, severe adverse effects or side effect (particle related) in this time frame.

Summary

The overall objective of our program is to develop medical capability to visualize blood clots in critical vessel locations that mark high risk for TEE. Such capability will open a new opportunity for clinicians to monitor disease risks and progression prior to events. Our technology offers new diagnostic criteria for disease staging and risk stratification, which in turn will result in more appropriate treatment algorithms. The data provided in this manuscript strongly suggest that a single systemic injection of FNDP-(NV)-Z~800 nm is safe and well tolerated. No indices of liver function abnormalities could be traced in spite of the long residency of particles in the liver. Further studies conducted by GLP formats, guided by FDA as IND qualification studies, will be needed to commence Phase I human clinical studies.

Acknowledgment

This study was supported in part by Debina Diagnostics Inc. and a research Bridge Funding Award (PIL) from the office of the vice president of Research Administration of Temple University.

Disclosure

The authors report no conflicts of interest in this work.

References

1. Benjamin EJ, Virani SS, Callaway CW, et al; American Heart Association Council on Epidemiology and Prevention Statistics Committee and Stroke Statistics Subcommittee. Heart disease and stroke Statistics-2018 update: a report from the American Heart Association. *Circulation*. 2018;137(12):e67–e492.
2. Dieleman JL, Baral R, Birger M, et al. US spending on personal health care and public health, 1996–2013. *JAMA*. 2016;316(24):2627–2646.
3. Feigin VL, Forouzanfar MH, Krishnamurthi R, et al; Global Burden of Diseases, Injuries, and Risk Factors Study 2010 (GBD 2010) and the GBD Stroke Experts Group. Global and regional burden of stroke during 1990–2010: findings from the global burden of Disease Study 2010. *Lancet*. 2014;383(9913):245–255.
4. Sidney S, Quesenberry CP, Jaffe MG. Recent trends in cardiovascular mortality. *JAMA Cardiol*. 2016;1(5):594–599.
5. Falk E. Pathogenesis of atherosclerosis. *J Am Coll Cardiol*. 2006; 47(8 Suppl):C7–C12.
6. North American Symptomatic Carotid Endarterectomy Trial Collaborators; Barnett HJM, Taylor DW, et al. Beneficial effect of carotid endarterectomy in symptomatic patients with high-grade carotid stenosis. *N Engl J Med*. 1991;325(7):445–453.
7. Barnett HJ, Taylor DW, Eliasziw M, et al. Benefit of carotid endarterectomy in patients with symptomatic moderate or severe stenosis. North American Symptomatic Carotid Endarterectomy Trial Collaborators. *N Engl J Med*. 1998;339(20):1415–1425.
8. Saba L, Mallarini G. A comparison between NASCET and ECST methods in the study of carotids: evaluation using multi-detector-row CT angiography. *Eur J Radiol*. 2010;76(1):42–47.
9. Walker MD, Marler JR, Goldstein M et al. Endarterectomy for asymptomatic carotid artery stenosis. Executive Committee for the Asymptomatic Carotid Atherosclerosis Study. *JAMA*. 1995;273(18):1421–1428.
10. Farrell B, Fraser A, Sanfercock P, Slattery J, Warlow CP. Randomised trial of endarterectomy for recently symptomatic carotid stenosis: final results of the MRC European Carotid Surgery Trial (ECST). *Lancet*. 1998;351(9113):1379–1387.
11. Flaherty ML, Kissela B, Khoury JC, et al. Carotid artery stenosis as a cause of stroke. *Neuroepidemiology*. 2013;40(1):36–41.
12. Lovrencic-Huzjan A, Rundek T, Katsnelson M. Recommendations for management of patients with carotid stenosis. *Stroke Res Treat*. 2012; 2012(12):1–12.
13. Grant EG, Benson CB, Moneta GL, et al. Carotid artery stenosis: gray-scale and Doppler US diagnosis – Society of Radiologists in Ultrasound Consensus Conference. *Radiology*. 2003;229(2):340–346.
14. Marks SJ, Khera S. Cryptogenic stroke: making the management less cryptic. *Cardiol Rev*. 2016;24(4):153–157.
15. Fonseca AC, Ferro JM. Cryptogenic stroke. *Eur J Neurol*. 2015;22(4): 618–623.
16. Khatri P, Kleindorfer DO, Devlin T, et al; PRISMS Investigators. Effect of alteplase vs aspirin on functional outcome for patients with acute ischemic stroke and minor nondisabling neurologic deficits: the prisms randomized clinical trial. *JAMA*. 2018;320(2):156–166.
17. Savitz SI, Baron JC, Yenari MA, Sanossian N, Fisher M, Midori A. Reconsidering neuroprotection in the reperfusion era. *Stroke*. 2017;48(12): 3413–3419.
18. Kamel H, Longstreth WT, Tirschwell DL, et al. The atrial cardiopathy and antithrombotic drugs in prevention after cryptogenic stroke randomized trial: rationale and methods. *Int J Stroke*. 2019;14(2):207–214.
19. Akobeng AK, Abdelgadir I, Boudjemline Y, Hijazi ZM. Patent foramen ovale (PFO) closure versus medical therapy for prevention of recurrent stroke in patients with prior cryptogenic stroke: a systematic review and meta-analysis of randomized controlled trials. *Catheter Cardiovasc Interv*. 2018;92(1):165–173.
20. Darmoch F, Al-Khadra Y, Soud M, Fanari Z, Alraies MC. Transcatheter closure of patent foramen ovale versus medical therapy after cryptogenic stroke: a meta-analysis of randomized controlled trials. *Cerebrovasc Dis*. 2018;45(3–4):162–169.
21. Marcinkiewicz C, Gerstenhaber JA, Mark Sternberg M, Lelkes PI, Feuerstein G. Bitistatin-functionalized fluorescent nanodiamond particles specifically bind to purified human platelet integrin receptor αIIbβ3 and activated platelets. *Int J Nanomedicine*. 2017;12:8471–8482.
22. Gerstenhaber JA, Barone FC, Marcinkiewicz C, et al. Vascular thrombus imaging in vivo via near-infrared fluorescent nanodiamond particles bioengineered with the disintegrin bitistatin (part II). *Int J Nanomedicine*. 2017;12:8471–8482.
23. Barone FC, Marcinkiewicz C, Li J, et al. Pilot study on biocompatibility of fluorescent nanodiamond-(NV)-Z~800 particles in rats: safety, pharmacokinetics, and bio-distribution (part III). *Int J Nanomedicine*. 2018;13:5449–5468.
24. Zhou J, Zhuang J, Li J, et al. Long-term post-stroke changes include myelin loss, specific deficits in sensory and motor behaviors and complex cognitive impairment detected using active place avoidance. *PLoS One*. 2013;8(3):e57503.
25. Zhou J, Li J, Rosenbaum DM, et al. The prolyl 4-hydroxylase inhibitor GSK360A decreases post-stroke brain injury and sensory, motor, and cognitive behavioral deficits. *PLoS One*. 2017;12(9):e0184049.
26. Chanut F, Kimbrough C, Hailey R, et al. Spontaneous cardiomyopathy in young Sprague-Dawley rats: evaluation of biological and environmental variability. *Toxicol Pathol*. 2013;41(8):1126–1136.
27. Barthold SW. Chronic progressive nephropathy in aging rats. *Toxicol Pathol*. 1979;7(1):1–6.
28. Purtov K, Petunin A, Inzhevatkin E, et al. Biodistribution of different sized nanodiamonds in mice. *J Nanosci Nanotechnol*. 2015;15(2): 1070–1075.
29. Moore L, Yang J, Lan TT, et al. Biocompatibility assessment of detonation nanodiamond in non-human primates and rats using histological, hematologic, and urine analysis. *ACS Nano*. 2016;10(8):7385–7400.

30. Rojas S, Gispert JD, Martín R, et al. Biodistribution of amino-functionalized diamond nanoparticles. In vivo studies based on 18F radionuclide emission. *ACS Nano*. 2011;5(7):5552–5559.
31. Bhattacharya K, Mukherjee SP, Gallud A, et al. Biological interactions of carbon-based nanomaterials: from coronation to degradation. *Nanomedicine*. 2016;12(2):333–351.
32. Andersson B, Thurnherr T, Kunzmann AA. Toxicology of engineered nanomaterials: focus on biocompatibility, biodistribution and biodegradation. *Biochim Biophys Acta*. 1810(3);2011:361–373.
33. Mochalin VN, Shenderova O, Ho D, Gogotsi Y. The properties and applications of nanodiamonds. *Nat Nanotechnol*. 2012;7(1):11–23.
34. Vaijayanthimala V, Cheng PY, Yeh SH, et al. The long-term stability and biocompatibility of fluorescent nanodiamond as an in vivo contrast agent. *Biomaterials*. 2012;33(31):7794–7802.
35. Monopoli MP, Åberg C, Salvati A, Dawson KA. Biomolecular coronas provide the biological identity of nanosized materials. *Nat Nanotechnol*. 2012;7(12):779–786.
36. Kelly PM, Åberg C, Polo E, et al. Mapping protein binding sites on the biomolecular corona of nanoparticles. *Nat Nanotechnol*. 2015;10(5):472–479.
37. Hamad-Schifferli K. Exploiting the novel properties of protein coronas: emerging applications in nanomedicine. *Nanomedicine (Lond)*. 2015;10(10):1663–1674.